applied sciences

MDPI

Article

Underwater In Situ Local Heat Treatment by Additional Stitches for Improving the Weldability of Steel

Jacek Tomków [1,*] and Anna Janeczek [2]

[1] Department of Materials Engineering and Welding, Faculty of Mechanical Engineering, Gdańsk University of Technology, G. Narutowicza 11/12, 80-233 Gdańsk, Poland

[2] Department of Materials Engineering and Welding, Gdańsk University of Technology, G. Narutowicza 11/12, 80-233 Gdańsk, Poland; ania.janeczek96@gmail.com

* Correspondence: jacek.tomkow@pg.edu.pl; Tel.: +48-58-347-1863

Received: 13 February 2020; Accepted: 4 March 2020; Published: 6 March 2020

Abstract: In this paper the influence of in situ local heat treatment performed by additional stitches on the weldability of high-strength low-alloy (HSLA) S355J2C+N steel was tested. The investigated steel is characterized by high susceptibility to cold cracking. It is necessary to find a method to improve the quality of welded joints. The local heat treatment was applied as an effect of bead-on plate welding made on the face of a Tekken test joint. The specimens were made by the use of covered electrodes in the water environment. For testing weldability, Tekken test specimens were made. Then, the different number of the pad welds with different overlapping were laid on the face of the tested welds. Non-destructive (NDT) visual and penetrant tests were undertaken. During the NDT, imperfections like shape mistakes and spatters were found. Then, metallographic macro- and microscopic testing were performed. The macroscopic observations proved that water environment can generate imperfections like cracking and pores. However, for specimens with additional stitches the number of imperfections decreased. Microscopic tests proved that the proposed technique affected the structure of the heat-affected zone (HAZ). The specimens without the application of additional stitches are characterized by brittle bainitic and martensitic structure. Specimens, in which the additional stitches were applied, contain tempered martensite, fine ferrite and fine pearlite in their HAZ. It was also observed that the number of cracks decreased for in situ local heat-treatment specimens. The final step was Vickers HV10 hardness measurement. These measurements confirmed previous results. The heat from additional stitches affected the steel by significantly decreasing the hardness by 80–100 HV10. The results of experiments showed that the heat from pad welds provided microstructural changes in heat-affected zones and a decrease in the susceptibility to cold cracking, which results in improvement in the weldability of HSLA steel in wet welding conditions.

Keywords: underwater wet welding; high-strength low-alloy steel; cold cracking; bead-on plate welding; metallographic testing

1. Introduction

High-strength low-alloy (HSLA) steels are used in many types of structure. In comparison to conventional low-carbon steels, HSLA steels are characterized by favorable strength-to-weight ratio. That results in a lower cost of structures [1]. The usage of these materials has been changing in recent years. Earlier, they have been used only in the air. Now, they are the most common materials used for marine structures, which are characterized by direct contact with water [2]. The following application may be classified as an example of marine and offshore structures:

- bridges [3];
- pipelines [4,5];
- wind turbines [6];
- ships [7];
- wharfs [8].

Defects could occur in marine and offshore structures, so it is important to find the proper strengthening technique [9]. The technique could be applied during preparation of the structures. The laying of the coating is widely used to improve the surface and properties of the substrate. Coatings are widely deposited by pad welding [10] and arc spraying [11]. The other method of improving the properties of the material surfaces could be the use of the ceramic brush tools to change the roughness. High roughness can generate the notch effect, which can cause a cracking effect [12]. Also, welding imperfections may occur in offshore constructions. During preparation of the structure, numerical analysis can be used for prediction the potential location of the failure [13,14]. Welding of HSLA steels in the air is a well-known process. There is a lot of literature addressing concerns about joining of these group of materials by different welding methods. To improve the quality of welded joints, the modeling of temperature field during multi-pass gas metal arc welding (GMAW) surfacing or rebuilding of steel elements taking into account that the heat of the deposit metal could be applied [15]. The cooling time between temperatures 800 °C and 500 °C (t8/5) is a factor with high influence on the quality of the joint [16]. This factor is responsible for microstructural transformations in a welded joint. There are HSLA steels in which the preheating process generates positive effects and provides increasing t8/5, which is responsible for decreasing the occurrence of the welding imperfections [17]. During joining in the air, the quality of a welded joint also depends on welding parameters [18] and filler material storage conditions [19].

However, offshore structures may undergo failures. Damaged areas can be located under the water surface, which determines the necessity of repairs in water conditions. There are three methods of underwater welding [20–23]:

- dry welding (hyperbaric and isobaric)—the welding area and welder are isolated from the environment by a special chamber;
- local dry cavity welding—the welding area is in situ isolated from environment, the steel plates and welder are in direct contact with environment;
- wet welding—the welding area and welder are in direct contact with the water environment.

The method of underwater welding used most often is wet welding. The most common methods of wet welding are flux-cored arc welding (FCAW) [24] and manual metal arc welding (MMA) [25,26]. The water, as a welding environment, generates problems, which have a negative influence on the quality of the joint. The biggest negative phenomenon during wet welding is presence of high diffusible hydrogen content in deposited metal. The results of the measurements of diffusible hydrogen in deposited metal ranged from 32.61 to 39.95 mL/100 g for specimens welded in air and from 51.50 to 61.34 mL/100 g for specimens made in the water [27]. This chemical element is a factor with significant impact on the properties of welded joints. A phenomenon of hydrogen embrittlement is characteristic for low-carbon structural steel also in the air [28,29]. This type of embrittlement can occur even with the cathodic protection conditions [30]. In an air environment, the modeling of a hydrogen-inducted delayed intergranular fracture in high strength steels can be used [31]. However, the prediction of diffusible hydrogen content in deposited metal, in a water environment, is impossible due to unpredictable process conditions, which change during welding. These changes result from the instability of the welding arc in the water, which is the other problem in this environment. Wang et al. stated that ultrasonic wave-assisted during underwater FCAW welding has the potential to control the dynamic bubble and then improve arc stability [32]. Xu et al. [33] proved, that droplet has significant influence on the stability of underwater welding process. Chen et al. [34] stated also that ultrasonic

energy decreases the porosity and diffusible hydrogen content, which can improve the quality of underwater welded joints.

Problems of underwater wet welding generate the high susceptibility of HSLA steel to cold cracking. The cold cracks can occur in the welds and in the heat-affected zone (HAZ) near the fusion line [35].

There are a couple of methods which provide to decreasing the susceptibility to cold cracking of underwater wet-welded joints. It was proved that welding with austenitic consumables, which provides welds with a good plasticity, can reduce the susceptibility to cold cracking. The temper bead welding can also decrease the number of cold cracks in pad welds, made in the water [25]. In previous experiments the bead sequence was investigated. It was stated that a proper bead sequence during underwater wet welding can contribute to decreasing the hardness, tempering the HAZ and reducing the number of cracks in the area of pad welds [36]. A further method reducing the susceptibility to cold cracking is submerged-arc welding applied to marine steels. Han et al. proved, that this method can also reduce the tendency to corrosion of underwater welded joints [37]. Wang et al. proposed welding with higher heat input, which provides a large possibility for a better protective effect and a larger weld penetration [38]. Another method for improving the quality of underwater welded joints is modification of filler materials. Menezes et al. [39] proposed silicate and polymer agglomerated electrodes, which caused higher arc voltage values in comparison to the conventional electrode with the same polarity. This may contribute to decreasing of the number of cracks in the welded joints, which results from lower diffusible hydrogen content in the deposited metal.

The use of traditional heat treatment possibilities is very limited in water due to the negative influence of the environment. Zhang et al. [40] proposed real-time induction heating during wet FCAW welding. Authors stated that the addition of induction heating could reduce the cooling rate of the joint in a water environment to improve the microstructural properties of the joint. The content of brittle structures such as martensite and bainite decreased while the proeutectoid ferrite and acicular ferrite phases increased. However, the induction heating process caused major problems with the stability of the welding arc. This can affect the quality of the welded joints. The local heat treatment as an effect of multiple passes has a positive effect in HSLA steels in air [41]. However, this method has not been verified sufficiently in a water environment.

The aim of this research was to study the influence of in situ local heat treatment on the weldability of high-strength low-alloy S355J2C+N steel. As a method for improving the weldability of steel local heat treatment, provided by the heat from additional stitches, was chosen. Weldability tests are commonly used to evaluate the possibilities of the welding in the air for different materials [42,43], and in the water [35]. A Tekken weldability test was chosen for investigation. This test allows assessment of the weldability for a butt-welded joint. On the basis of performed tests [44], it was concluded that investigated S355J2C+N steel is characterized by good weldability during welding in the air and poor in underwater conditions. S355J2C+N steel is widely used in offshore structures, which might be needing a repairs in the water. To the best of the author's knowledge, there is no research in the literature that provided detailed discussion on the improvement the weldability of a HSLA steel butt-welded joint made in the wet welding conditions.

2. Materials and Methods

2.1. Used Materials

The HSLA S355J2C+N steel (16 mm thick) was chosen as a base material (BM) for welding. The chemical composition of investigated steel has been analyzed by the emission spectrometry method with spark excitation. As a filler material, ISO 2560-A: E 38 0 R11 [45] rutile electrodes (4.0 diameter) were used, which provide welds with a good plasticity, which contributes to decreasing susceptibility to cold cracking. The chemical composition of the used materials are presented in Table 1. The mechanical properties as yield point (R_e) and tensile strength (R_m) of filler materials should be

equal or greater than the properties of BM [41]. However, the filler material is characterized by a higher value of elongation (A_5), to decrease the susceptibility to cold cracking [25]. The mechanical properties of the used materials are listed in Table 2.

Table 1. Chemical composition of used materials wt. %.

Material	C	Si	Mn	P	Cr	Mo	Ni	Cu	V	Ce_{IIW} [1]
S355J2C+N in accordance to control analysis	0.20	0.50	1.10	0.02	0.02	0.001	0.001	0.02	0.005	0.386
E 38 0 R 11 electrodes deposit in accordance to manufacturer data	0.07	0.44	0.55	0.01	0.04	-	-	0.05	-	-

[1] Ce_{IIW}—carbon equivalent by International Institute of Welding.

Table 2. Mechanical properties of used materials in accordance to manufacturer data.

Material	Yield Point, R_e (MPa)	Tensile Strength, R_m (MPa)	Elongation, A_5 (%)
S355J2C+N	min. 355	470–630	17–22
E 38 0 R 11 electrodes deposit	503	538	26

2.2. Welding Procedure

In accordance with EN-ISO 17642-2 [46] the Tekken weldability test was chosen for the experiment. This test enables assessment of susceptibility to cold cracking in all joint areas. The Tekken test is one of the weldability tests, which is characterized by high thermal severity. This test was chosen because it allows us to study even a small impact of factors on weldability. For the experiment, six Tekken test were prepared. The upper surfaces of all specimens were placed 0.5 m below the water surface. The schematic view of the Tekken specimens is presented in Figure 1.

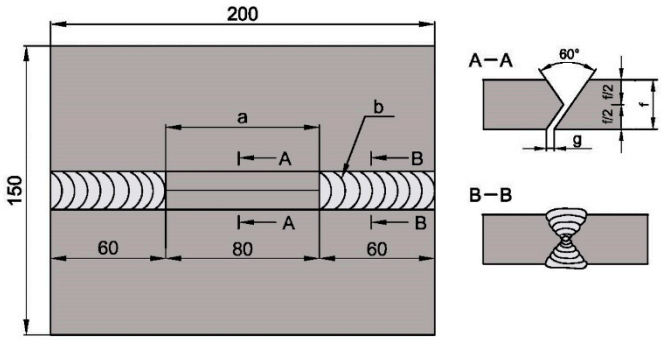

Figure 1. Schematic illustration of the Tekken test specimen.

In the first step of investigations, the Tekken butt welded joints were performed. The welding was carried out in the flat position in accordance to EN ISO 17642-2 standard [46]. In the next step five of the Tekken specimens were modified. On the surface of the prepared butt welded joints, the additional stitches were laid immediately after preparation of Tekken joints, to check the influence of the proposed technique on the HSLA steel weldability in wet-welding conditions. The in situ heat treatment was an effect of the heat impact generated by the process of welding of additional stitches. They were laid in the same direction as the Tekken test weld, within the maximum time of two minutes after completion of the previous welding process. The scientific hypothesis stated that this modification causes changes in microstructure in heat affected zone (HAZ), which decreases the hardness. The specimens were modified by applying one, two or three additional stitches to the face of the Tekken weld. The stitches were welded with different distance between axes of the stitches calculated as percentage overlapping. During the process, the welding arc was unstable, which produces difficulties in keeping the constant welding speed and planned overlapping of the stitches. One of the reasons was limited visibility of the welding area, which disturbed the process of welding. These factors are typical for underwater

wet-welding processes [25,27,36]. The welding parameters are presented in Table 3. The additional stitches were welded with higher heat input values in accordance with the literature proceedings [25]. The schematic view of cross-sections of the tested area of each specimen is shown in Figure 2.

Table 3. Welding conditions for tested specimens.

Specimen No.	Stitch No.	Overlapping (%)	I (A)	U (V)	ql (kJ/mm)
1	1	-	180	26.3	0.60
2	1	-	184	26.0	0.92
	2	100	200	28.0	0.91
3	1	-	184	27.3	0.76
	2	90	200	27.0	0.86
4	1	-	188	25.0	0.80
	2	80	196	30.0	0.95
5	1	-	180	25.0	0.68
	2	100	200	29.0	0.65
	3	100	200	28.8	0.64
6	1	-	180	27.3	0.59
	2	100	200	27.5	0.81
	3	100	200	27.8	0.97
	4	10	204	28.0	0.90

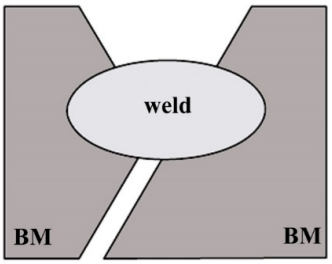

(a)

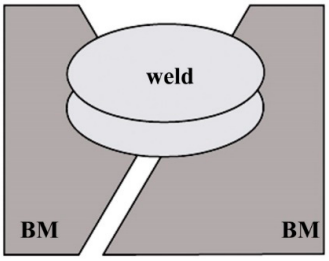

(b)

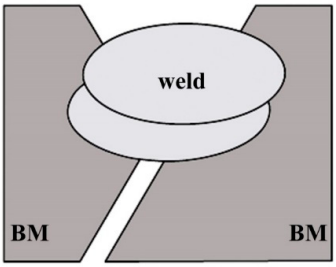

(c)

Figure 2. *Cont.*

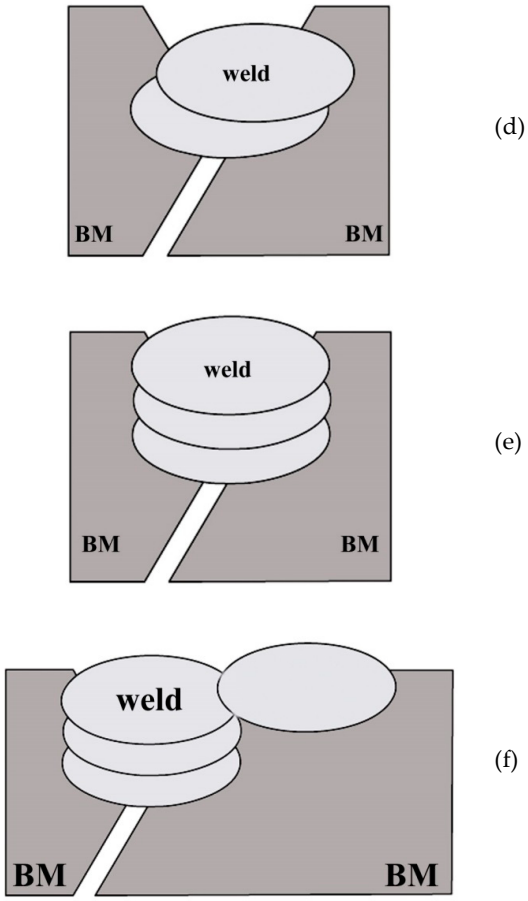

Figure 2. The schematic view of cross-sections of tested areas: (**a**) Specimen 1; (**b**) Specimen 2; (**c**) Specimen 3; (**d**) Specimen 4; (**e**) Specimen 5; (**f**) Specimen 6.

2.3. Methodology of the Tests

Tekken joints were tested by non-destructive tests (NDT) and destructive tests (DT). The first step was NDT: visual testing (VT) in accordance with the EN ISO 17637:2017 [47] standard and penetrant testing (PT) in accordance with the EN ISO 3452-1:2013 standard [48]. After NDT specimens were cut for DT at $\frac{1}{4}$, $\frac{1}{2}$, and $\frac{3}{4}$ of joint length of each specimens, and from each specimen, two testing specimens were chosen. The prepared cross-sections were grinded, polished, and etched by Nital 4%. Then, the metallographic macro-and microscopic testing was undertaken in accordance with the EN ISO 17639:2013 standard [49]. For micro observations optical microscope was used. Finally, Vickers HV10 measurements were undertaken in accordance with the EN ISO 9015-1:2011 standard [50]. The first stitch (Tekken test weld) joined two pieces of used steel. The additional stitches, which were laid on the surface of previous stitches provided the heat, which caused local heat treatment of lower areas of the joint. The measurement points were located near the first welded stitch to show the influence of the local in situ heat treatment on the microstructure of HAZ and hardness in this area. The hardness was measured in the weld and HAZ in both sides from the axes of joint.

3. Results and Discussion

3.1. Non-Destructive Testing (NDT)

As previous investigations showed [44], used S355J2C+N steel is characterized by high susceptibility to cold cracking. Those cracks can occur 72 h after welding. The NDT was prepared after this time. During NDT some imperfections such as shape mistakes and spatters were found.

The results of NDT allowed us to mark areas for DT without surface imperfections. The exemplary results of NDT are presented in Figure 3.

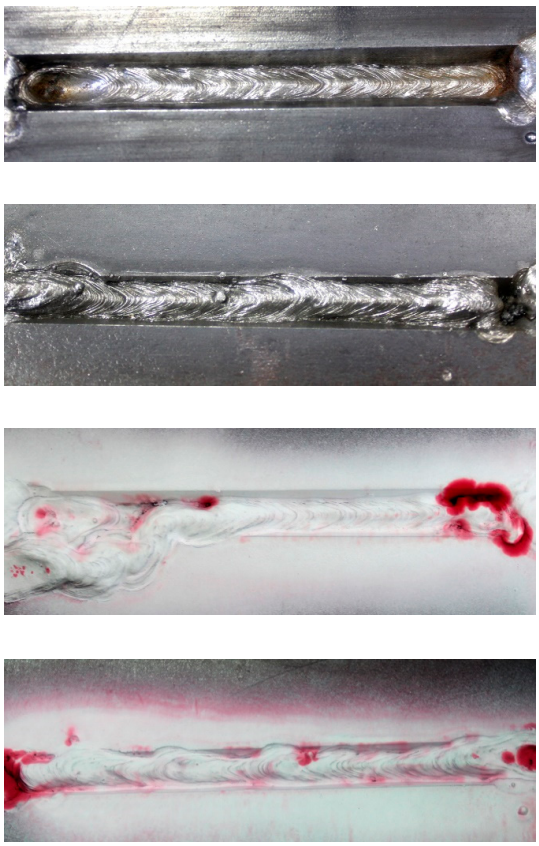

Figure 3. The exemplary results of non-destructive testing (NDT): (**a**) VT of Specimen 1; (**b**) visual testing (VT) of Specimen 3; (**c**) PT of Specimen 2; (**d**) penetrant testing (PT) of Specimen 5.

3.2. Metallographic Macroscopic Testing

The macroscopic tests showed the significant differences in cross-sections of prepared specimens. Specimen 1 welded without additional stitches (in-situ local heat treatment) was broken into two parts through a fusion line (FL). It was proved that S355J2C+N steel is characterized by high susceptibility to cold cracking. In specimen 1 the gas pore in the weld was found (Figure 4a). Specimens in which the additional stitches were laid were not broken into two parts. However, in Specimen 2, in which the overlapping was 100%, the crack was found. This crack started near the notch and ran through the FL into weld. The length of this crack was 90% of the weld height (Figure 4b). In other specimens no imperfections were found. The exemplary, representative photos of macroscopic testing are presented in Figure 4.

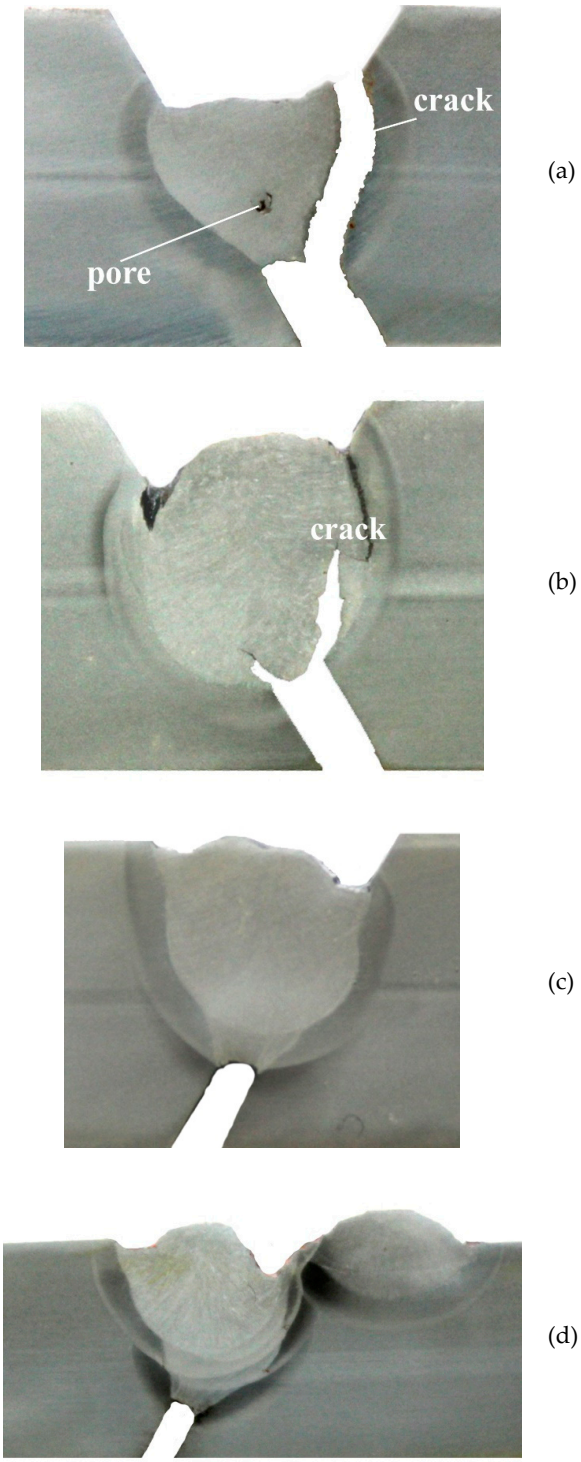

Figure 4. The exemplary results of macroscopic testing: (**a**) Specimen 1; (**b**) Specimen 2; (**c**) Specimen 5; (**d**) Specimen 6.

3.3. Metallographic Microscopic Testing

From each welded joint two specimens were observed using an optical microscope. The observations were carried out in the weld, in BM and in HAZ. The microstructure of S355J2C+N steel is characterized by the presence of fine-grained ferrite and fine-grained pearlite (Figure 5a). The structure of the weld, which was not tempered by heat from additional stitch was the same in each specimen. The dendritic structure was built of bright fine-grained ferrite arranged in columns,

from which grew acicular ferrite at the boundaries of dendrites. Inside dendrites were fine grains of ferrite, which is typical for weld made under water (Figure 5b) [25,27,36]. The structures in HAZ were different in each specimen. Specimen 1 welded without the additional stitches was characterized by brittle, martensitic and bainitic structures (Figure 5b). The observed brittle structures are the result of a high cooling rate generated by the water environment. Zhang et al. [40] stated that these structures cause decreasing of the mechanical properties of underwater welded joints, and may increase the susceptibility to cracking. The structures in HAZ in Specimen 2 were similar. The application of additional stitch with the 100% overlapping did not affect changes of microstructures in the HAZ, which generated cracks near the FL (Figure 5c). Similar results were found by Tasak et al. [51]. They proved, that in some applications, the structure after heat treatment did not change, and still included brittle martensite. Significant changes were observed in the weld of next specimens in areas where the heat from the additional stitch was affected. These areas were characterized by disappearance of the dendritic structure and the formation of a ferritic fine-grained structure (Figure 5d). The changes in overlapping of tempering stitch contributes to tempering the brittle martensitic structure in the HAZ. The structure in this area was mixed of brittle martensite, tempered martensite, ferrite and pearlite (Figure 5e). The 80% overlapping provided a higher content of tempered structures in the HAZ. However, cracks were still observed (Figure 5f). Using two tempering stitches with 100% overlapping (Specimen 5) provided the best results. The in situ local heat treatment generated the normalization structures with fine pearlite and fine ferrite in areas overlapping the HAZ from base stitch and tempering stitches (Figure 5g). It was proved that the temper bead welding technique is able to stop the cracking by the change of structure in bead-on plate welding conditions [52]. The additional stitches were laid in the same direction as the Tekken test weld, within the maximum time of two minutes after competition of previous welding process. It allows to increase the cooling rate of prepared specimens. Sun et al. [53] performed an experiment with in situ quench and tempering for microstructure control and enhanced the mechanical properties of a laser cladded process. They proved that by pausing 80 s between tracks, a partial tempering effect was achieved. In this paper, we achieved a similar tempering effect of the structures in HAZ. Jorge et al. [54] proved that longer cooling times show a tendency to improvement of impact toughness of high-strength steel weld metals obtained by GMAW process. It can be assumed that our technique would also improve the mechanical properties. The microstructure in the area of overlapping of three HAZ in Specimen 5 was the same as in Specimen 6 in the area where the third additional stitch with 10% overlapping generated in situ heat treatment (Figure 5h). The structure in this area was built by normalized structures with fine pearlite and fine ferrite. The microstructure in HAZ (which did not overlap on the other HAZ) in the last stitch is similar to the microstructure of the HAZ for Specimen 1 (without in situ local heat treatment). This stitch provided the heat treatment of the previous laid stitches. In industrial applications, the last stitch can be ground after completion of the welding process. Water as a welding environment causes a high cooling rate of welded joints. The residual thermal stresses are generated as a result of the decreasing of t8/5 time. Rahman Rashid et al. [55] proved that micro-cracking in the welds near the surface of the clads is developed by high rates of surface solidification in air environment. The solidification rate of the welds in the water is quicker, and caused the susceptibility to cracking in the weld. This may be the reason for the cracks observed in the weld (Figure 5i) of Specimen 6. The exemplary results of metallographic microscopic testing are presented in Figure 5.

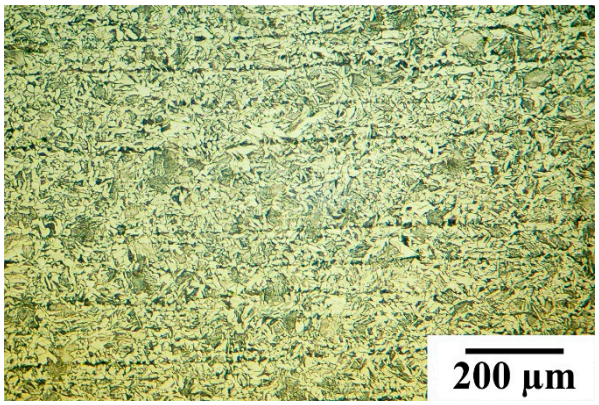

(a)

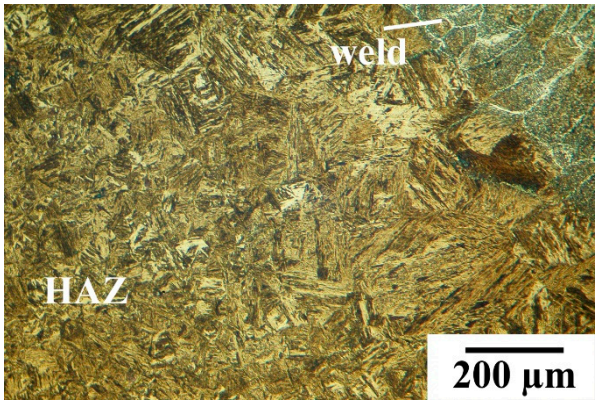

(b)

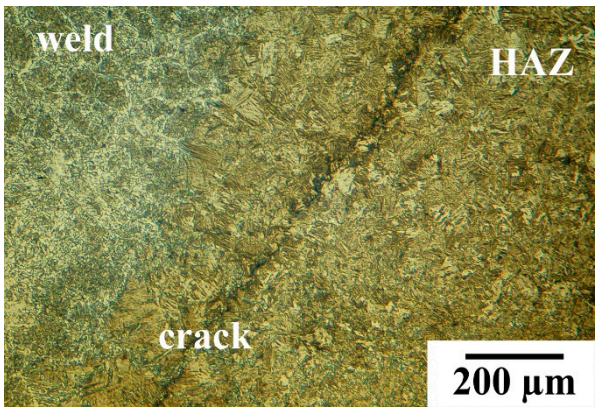

(c)

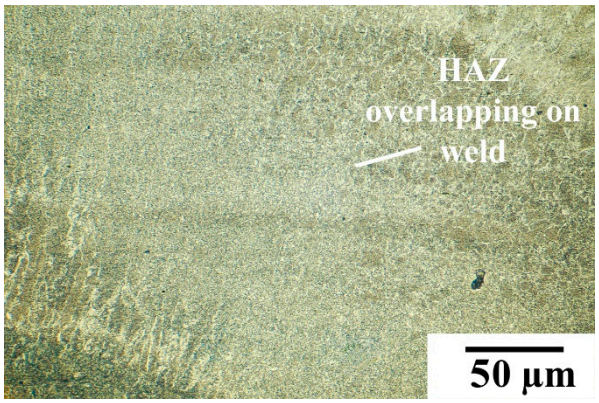

(d)

Figure 5. *Cont.*

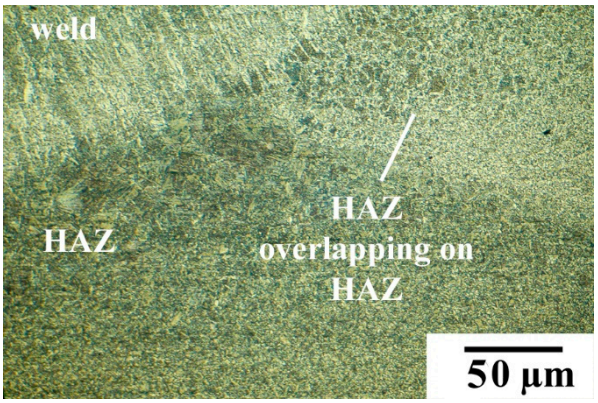

(e)

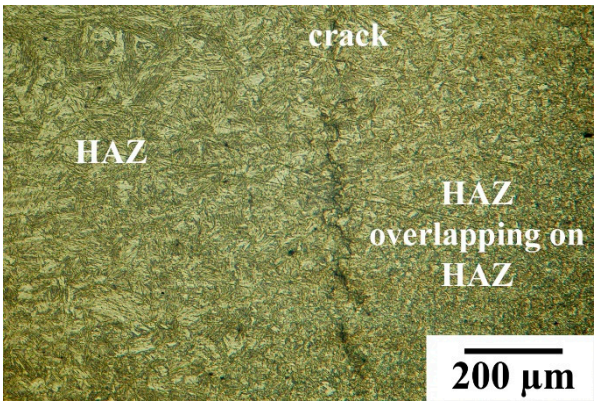

(f)

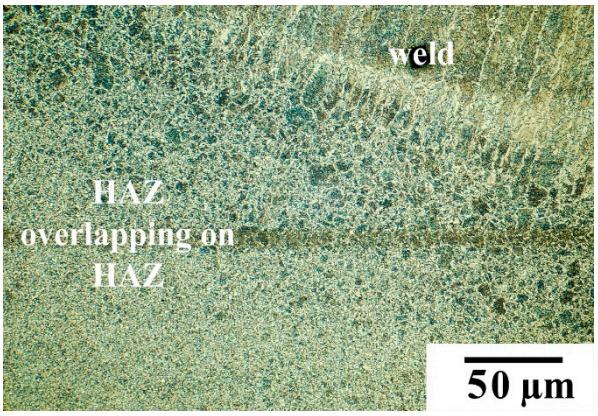

(g)

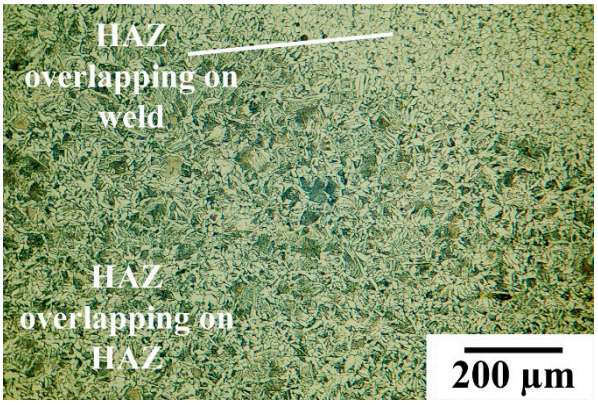

(h)

Figure 5. *Cont.*

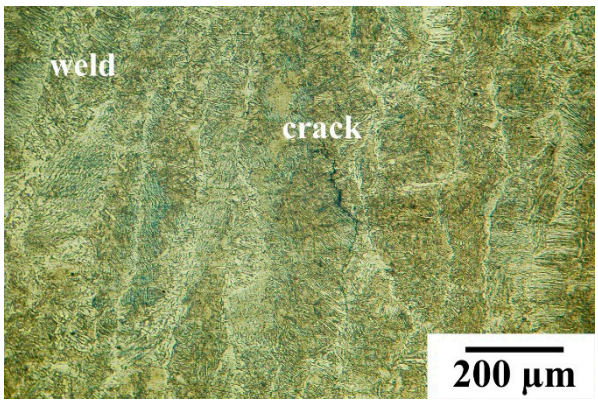

(i)

Figure 5. The exemplary results of microscopic testing: (**a**) S355J2C+N structure; (**b**) Specimen 1 without in situ heat treatment—the view of the weld and heat-affected zone (HAZ); (**c**) Specimen 2, one additional stitch with 100% overlapping—the view of the weld and HAZ; (**d**) Specimen 3, one additional stitch with 90% overlapping—the view of the tempered weld and HAZ; (**e**) Specimen 3, one additional stitch with 90% overlapping—the view of the tempered HAZ; (**f**) Specimen 4, one additional stitch with 80% overlapping—the view of the weld and HAZ; (**g**) Specimen 5, two additional stitches with 100% overlapping—the view of the tempered HAZ; (**h**) Specimen 6, three additional stitches with 10% overlapping of the las—the view of the tempered HAZ t; (**i**) Specimen 6, three additional stitches with 10% overlapping of the last stitch—the view of the weld.

3.4. Hardness HV10 Measurements

For hardness HV10 measurements, the Sinowon V-10 stand (Sinowon, Dongguan, China) was used. The hardness was measured in three points in the weld and in six points in the HAZ—three in the left side from the axis of tested specimen and three in right side. Measurements were undertaken in two cross-sections of each specimen (e.g., 1.1. and 1.2. for Specimen 1). Rahman Rashid et al. [56] proved that decreasing hardness can result from tempered martensite occurring in the HAZ. The same results were observed during our investigation. Hardness HV10 measurements confirmed the microscopic observations. The highest HV10 values were measured in the HAZ, whose structures were identified as brittle bainitic and martensitic structure. Lisiecki and Ślizak [57] stated, that high hardness of welded layers was caused by a high cooling rate during welding process. The significant effect of in situ local heat treatment was observed for Specimen 5, modified by two additional stitches. The hardness HV10 values in this Specimen in HAZ were lower by 70–90 compared to the Specimen 1, which was performed without additional stitches. The proposed technique caused decreasing of the hardness in HAZ on both sides of weld axis. In Specimen 5, the biggest tempering effect was observed during microscopic testing. For Specimens 4 and 6, where an additional stich was non symmetrical, the hardness decreased in heat treatment areas (HAZ on right side from weld axis). The aim of using such a low value of overlapping like in Specimen 6 (10%) was tempering the area near the edge to check the influence of this value on the weldability of HSLA steel. The prepared examinations confirmed that 10% overlapping caused microstructural changes and a decrease of hardness in the HAZ of Tekken test weld. It proved that the applied method of in situ local heat treatment can be used during underwater welding as a technique, which improved the weldability of the HSLA steel in wet welding conditions. However, it was observed that overlapping higher than 80% of one stitch generated higher hardness and should be avoided. The results of HV10 hardness measurements are presented in Table 4. The hardness distribution in each specimens is presented in Figure 6.

Table 4. The results of HV10 hardness measurements.

Specimen No.	Heat Affected Zone (HAZ)			Base Material (BM)			HAZ		
1.1.	416	493	491	281	271	260	464	432	426
1.2.	475	458	423	262	275	276	446	451	428
2.1.	491	499	489	259	274	258	497	452	493
2.2.	479	465	439	258	266	242	472	471	477
3.1.	450	499	493	255	238	287	474	475	475
3.2.	482	501	472	260	245	278	404	466	430
4.1.	455	462	419	210	220	225	415	396	401
4.2.	461	452	459	260	286	232	384	371	379
5.1.	428	367	386	261	284	271	394	398	409
5.2.	381	390	382	266	265	284	373	384	378
6.1.	494	486	490	254	258	262	394	408	402
6.2.	480	494	490	277	280	275	387	367	377

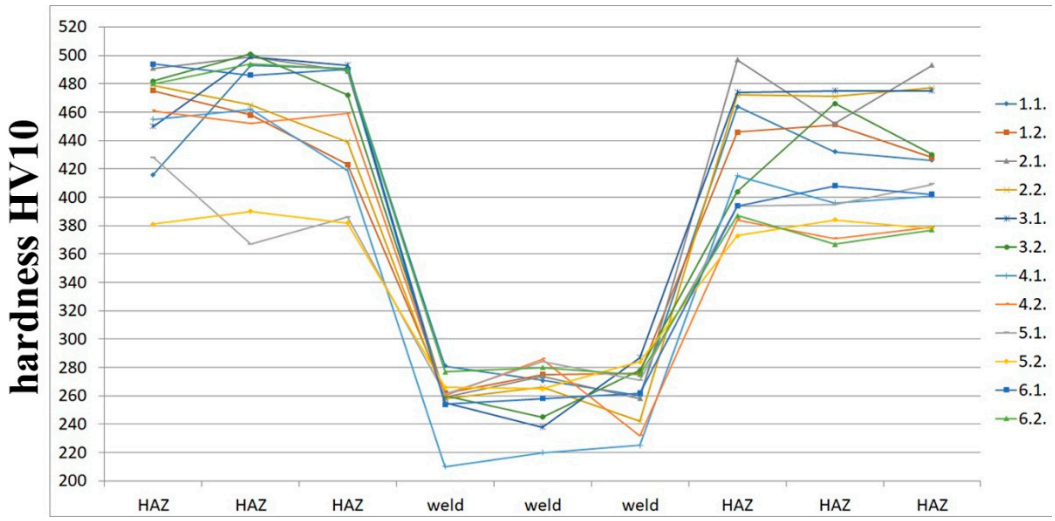

Figure 6. The distribution of hardness HV10 measurements for all specimens.

The effect of decreasing of HV10 hardness due to in situ local heat treatment can be observed in areas where heat from additional stitch tempered the microstructures of the base Tekken test joint. The measurements showed that there are significant differences in HAZ on both sides of the Tekken joint. These differences resulted from different heat influence on the joint. In the HAZ near the additional stitch (Specimens 4 and 6) the heat provides microstructural changes, which produced lower hardness. The HAZ on other side from the weld axis have not been tempered as much and the hardness is similar to the hardness in Specimen 1 welded without in situ heat treatment. Alipooramirabad et al. [58] proved that hardness level in the welded joint can be related to the microstructure constituent of bainite and Widmanstäten ferrite. These type of structures were observed during our microscopic testing in specimens, which are characterized by the highest HV10 hardness values. For Specimen 5, in which the additional stitch was produced by bead-on plate conditions with the 100% overlapping, the heat was implemented symmetrically, which provided a decrease of the hardness values in the whole HAZ, which resulted from tempering the microstructure in this region.

4. Conclusions

In the paper the effect of in situ local heat treatment on the weldability of HSLA steel welded under water in wet welding conditions was studied. The investigations showed that additional stitches can improve the quality of welded joints in the water environment. The additional stitches provided microstructural changes in the HAZ, decreasing the hardness in this area. Prepared investigations showed that the optimal number of stitches with 100% overlapping for S355J2C+N steel welded in wet welding conditions is three.

The main conclusions resulting from experiments are:

1. The investigated S355J2C+N steel is characterized by poor weldability in wet welding conditions. The way to improve the weldability in the water environment is in situ local heat treatment provided by additional welded stitches. During non-destructive testing it was observed that these stitches do not cause imperfections on the surface.
2. The additional stitch laid on the face of welded joint contributed to tempering of brittle structures in heat-affected zones which generated lower values of HV10 hardness. The tempered martensite and normalized structures were observed during microscopic testing.
3. For improvement of the weldability of S355J2C+N steel in a water environment, two additional stitches with 100% overlapping should be laid. This technique generated normalized structures with fine pearlite and fine ferrite in the HAZ, which decrease hardness in this area by 70–90 HV10. The higher number of additional stitches provided microstructure changes in the welded joint, which may result from increasing the crucial t8/5 time.
4. The positive effect can also be achieved by bead-on plate welding with the one stitch with overlapping lower then 80%. Welding with higher values increased the hardness and did not affect the tempering of HAZ.

Author Contributions: Conceptualization, J.T.; methodology, J.T.; validation, J.T.; formal analysis, J.T.; investigation, J.T. and A.J.; writing—original draft preparation, J.T.; writing—review and editing, J.T. and A.J.; supervision, J.T.; All authors have read and agreed to the published version of the manuscript.

Funding: This research received no external funding.

Acknowledgments: Authors want to thank Dariusz Fydrych from Gdańsk University of Technology for the support and his guidance during our work.

Conflicts of Interest: The authors declare no conflict of interest.

References

1. Aleksić, V.; Milović, L.; Blacić, I.; Vuherer, T.; Bulatović, S. Effect of LCF on behavior and microstructure of microalloyed HSLA steel and its simulated CGHAZ. *Eng. Fail. Anal.* **2019**, *104*, 1094–1106. [CrossRef]
2. Den Besten, H. Fatigue criteria classification, modeling, developments and trends for welded joints in marine structures. *Ships Offshore Struct.* **2018**, *13*, 787–808. [CrossRef]
3. Hu, J. Application of long-distance microscope in crack detection in bridge construction. *Acta Microsc.* **2019**, *28*, 1151–1158.
4. Park, J.H.; Moon, H.S. Advanced automatic welding system for offshore pipeline system with seam tracking function. *Appl. Sci.* **2020**, *10*, 324. [CrossRef]
5. Bunaziv, I.; Olden, V.; Akselsen, O.M. Metallurgical aspects in the welding of clad pipelines–A global outlook. *Appl. Sci.* **2019**, *9*, 3118. [CrossRef]
6. Dirisu, P.; Ganguly, S.; Mehmanparast, A.; Martina, F.; Williams, S. Analysis of fracture toughness properties of wire + arc additive manufactured high strength low alloy structural steel components. *Mater. Sci. Eng. A* **2019**, *765*, 138285. [CrossRef]
7. Zhu, L.; Wang, Y.; Wang, S.; Zhang, Q.; Zhang, C. Research of microalloy elements to induce intragranular acicular ferrite in shipbuilding steel. *Ironmak. Steelmak.* **2019**, *46*, 499–507. [CrossRef]
8. Law, D.W.; Nicholls, P.; Christodoulou, C. Residual protection of steel following suspension om Impressed Current Cathodic Protection system on a wharf structure. *Constr. Build. Mater.* **2019**, *210*, 48–55. [CrossRef]
9. Dehghani, A.; Aslani, F. A review on defects in steel offshore structures and developed strengthening techniques. *Structures* **2019**, *20*, 635–657. [CrossRef]
10. Chmielewski, T.; Hudycz, M.; Krajewski, A.; Sałaciński, T.; Skowrońska, B.; Świercz, R. Structure investigation of titanium metallization coating deposited onto AlN ceramics substrate by means of friction surfacing process. *Coatings* **2019**, *9*, 845. [CrossRef]
11. Adamiak, M.; Czupryński, A.; Kopyść, A.; Monica, Z.; Olender, M.; Gwiazda, A. The properties of arc-sprayed aluminum coatings on armor-grade steel. *Metals* **2018**, *8*, 142. [CrossRef]
12. Sałaciński, T.; Chmielewski, T.; Winiarski, M.; Cacko, R.; Świercz, R. Roughness of metal surface after finishing using ceramic brush tools. *Adv. Mater. Sci.* **2018**, *18*, 20–27. [CrossRef]

13. Li, C.; Dong, S.; Wang, T.; Xu, W.; Zhou, X. Numerical investigation on ultimate compressive strength of welded stiffened plates built by steel grades of S235-S390. *Appl. Sci.* **2019**, *9*, 2088. [CrossRef]
14. Kik, T.; Moravec, J.; Nováková, I. Numerical simulations of X22CrMoV12-1 steel multilayer welding. *Arch. Metall. Mater.* **2019**, *64*, 1441–1448. [CrossRef]
15. Winczek, J. Modeling of temperature field during multi-pass GMAW surfacing or rebuilding of steel elements taking into account the heat of the deposit metal. *Appl. Sci.* **2016**, *7*, 6. [CrossRef]
16. Sajek, A.; Nowacki, J. Comparative evaluation of various experimental and numerical simulation methods for determination of t(8/5) cooling times in HPAW process weldments. *Arch. Civ. Mech. Eng.* **2018**, *18*, 583–591. [CrossRef]
17. Fu, H.; Xu, B.; Xiao, Q.; Li, S.; Zhang, X.; Bian, S.; Kang, T. Effect of preheating temperature on post-weld residual stress of dissimilar steel plates. *Metalurgija* **2020**, *59*, 150–152. Available online: https://hrcak.srce.hr/232360 (accessed on 6 March 2020).
18. Landowski, M. Influence of parameters of laser beam welding on structure of 2205 duplex stainless steel. *Adv. Mater. Sci.* **2019**, *19*, 21–31. [CrossRef]
19. Świerczyńska, A. Effect of storage conditions of rutile flux cored welding wires on properties of welds. *Adv. Mater. Sci.* **2019**, *19*, 46–56. [CrossRef]
20. Hu, Y.; Shi, Y.; Sun, K.; Shen, X. Effect of filler Si content on the microstructure and properties of underwater hyperbaric welded duplex stainless steel. *J. Mater. Process. Technol.* **2020**, *279*, 116548. [CrossRef]
21. Hu, Y.; Shi, Y.; Shen, X.; Wang, Z. Microstructure evolution and selective corrosion resistance in underwater multi-pass 2101 duplex stainless steel welding joints. *Metall. Mater. Trans. A* **2018**, *49*, 3306–3320. [CrossRef]
22. Guo, N.; Fu, Y.; Xing, X.; Liu, Y.; Zhao, S.; Feng, J. Underwater local dry cavity laser welding of 304 stainless steel. *J. Mater. Process. Technol.* **2018**, *260*, 146–155. [CrossRef]
23. Rogalski, G.; Fydrych, D.; Łabanowski, J. Underwater wet repair welding of API 5L X65M pipeline steel. *Pol. Marit. Res.* **2017**, *24*, 188–194. [CrossRef]
24. Yang, Q.; Han, Y.; Chen, J.; Dong, S.; Wu, C.; Jia, C. Visual investigation on the arc burning behaviors and features in underwater wet FCAW. *J. Offshore Mech. Arct. Eng.* **2020**, 1–22. [CrossRef]
25. Tomków, J.; Fydrych, D.; Rogalski, G.; Łabanowski, J. Temper bead welding of S460N steel in wet welding conditions. *Adv. Mater. Sci.* **2018**, *18*, 5–14. [CrossRef]
26. Tomków, J.; Czupryński, A.; Fydrych, D. The abrasive wear resistance of coatings manufactured on high-strength low-alloy (HSLA) offshore steel in wet welding conditions. *Coatings* **2020**, *10*, 219. [CrossRef]
27. Tomków, J.; Fydrych, D.; Rogalski, G.; Łabanowski, J. Effect of the welding environment and storage time of electrodes on the diffusible hydrogen content in deposited metal. *Rev. Metal.* **2019**, *55*, e140. [CrossRef]
28. Wasim, M.; Djukic, M.B. Hydrogen embrittlement of low carbon structural steel at macro-, micro-, and nano-levels. *Int. J. Hydrog. Energy* **2020**, *45*, 2145–2156. [CrossRef]
29. Rhode, M.; Richter, T.; Mayr, M.; Nitsche, A.; Mente, T.; Böllinghaus, T. Hydrogen diffusion in creep-resistance 9% Cr P91-multi-layer weld metal. *Weld. World* **2020**, *64*, 267–281. [CrossRef]
30. Świerczyńska, A.; Fydrych, D.; Landowski, M.; Rogalski, G.; Łabanowski, J. Hydrogen embrittlement of X2CrNiMoCuN25-6-3 super duplex stainless steel welded joints under cathodic protection. *Constr. Build. Mater.* **2019**, *238*, 117697. [CrossRef]
31. Wu, W.; Wang, Y.; Tao, P.; Li, X.; Gong, J. Cohesive zone modeling of hydrogen-inducted delayed intergranular fracture in high strength steels. *Results Phys.* **2018**, *11*, 591–598. [CrossRef]
32. Wang, J.; Sun, Q.; Zhang, T.; Tao, X.; Jin, P.; Feng, J. Arc stability indexes evaluation of ultrasonic wave-assisted underwater FCAW using electrical signal analysis. *Int. J. Adv. Manuf. Technol.* **2019**, *103*, 5–8. [CrossRef]
33. Xu, C.; Guo, N.; Zhang, X.; Chen, H.; Fu, Y.; Zhou, L. Internal characteristic of droplet and its influence on the underwater wet welding process stability. *J. Mater. Process. Technol.* **2020**, *280*, 116593. [CrossRef]
34. Chen, H.; Guo, N.; Xu, K.; Xu, C.; Zhou, L.; Wang, G. In-situ observations of melt degassing and hydrogen removal enhanced by ultrasonics in underwater wet welding. *Mater. Des.* **2020**, *188*, 108482. [CrossRef]
35. Fydrych, D.; Łabanowski, J.; Tomków, J.; Rogalski, G. Cold cracking of underwater wet welded S355G10+N high strength steel. *Adv. Mater. Sci.* **2015**, *15*, 48–56. [CrossRef]
36. Tomków, J.; Fydrych, D.; Rogalski, G. Role of bead sequence in underwater welding. *Materials* **2019**, *12*, 3372. [CrossRef] [PubMed]
37. Han, Y.; Dong, S.; Zhang, M.; Jia, C.; Zhang, M.; Wu, C. A novel underwater submerged-arc welding acquires sound quality joints for high strength marine steel. *Mater. Lett.* **2020**, *261*, 127075. [CrossRef]

38. Wang, J.; Sun, Q.; Zhang, T.; Xu, P.; Feng, J. Experimental study of arc bubble growth and detachment from underwater wet FCAW. *Weld. World* **2019**, *63*, 1147–1759. [CrossRef]
39. Menezes, P.; Pessoa, E.; Bracarense, A.Q. Comparison of underwater wet welding performed with silicate and polymer agglomerated electrodes. *J. Mater. Process. Technol.* **2019**, *266*, 63–72. [CrossRef]
40. Zhang, T.; Dai, X.; Feng, J.; Hu, L. Preliminary investigation on real-time induction heating-assisted underwater wet welding. *Weld. J.* **2015**, *94*, 8–15.
41. Rathod, D.W.; Sun, Y.; Obasi, G.C.; Roy, M.J. Effect of multiple passes on Lüders/yield plateaus, microstructure and tensile behavior of narrow-gap thick-section weld plates. *J. Mater. Sci.* **2019**, *54*, 12833–12850. [CrossRef]
42. Górka, J. Assessment of the weldability of T-welded joints in 10 mm thick TMCP steel using laser beam. *Materials* **2018**, *11*, 1192. [CrossRef] [PubMed]
43. Skowrońska, B.; Chmielewski, T.; Golański, D.; Szulc, J. Weldability of S700MC steel welded with the hybrid plasma + MAG method. *Manuf. Rev.* **2020**, *7*, 4. [CrossRef]
44. Tomków, J.; Janeczek, A. The influence of the welding environment on the properties of Tekken joints made from S355J2C+N steel. *Weld. Technol. Rev.* **2019**, *91*, 8–12. [CrossRef]
45. *A Classification of Coated Rod Electrodes for Arc Welding of Unalloyed Steel and Fine-Grained Steel*; ISO 2560; ISO: Geneva, Switzerland, 1908.
46. *Destructive Tests on Welds in Metallic Materials—Cold Cracking Tests for Weldments—Arc Welding Processes*; EN ISO 17642; ISO: Geneva, Switzerland, 2015.
47. *Non-Destructive Testing of Welds—Visual Testing of Fusion-Welded Joints*; EN ISO 17637; ISO: Geneva, Switzerland, 2017.
48. *Non-Destructive Testing—Penetrant Testing—Part 1: General Principles*; EN ISO 3452-1; ISO: Geneva, Switzerland, 2013.
49. *Destructive Tests on Welds in Metallic Materials. Macroscopic and Microscopic Examination of Welds*; EN ISO 17639; ISO: Geneva, Switzerland, 2013.
50. *Destructive Tests on Welds in Metallic Materials. Hardness Testing. Hardness Test on Arc Welded Joint*; EN ISO 9015-1; ISO: Geneva, Switzerland, 2011.
51. Tasak, E.; Ziewiec, A.; Zielińska-Lipiec, A.; Ziewiec, K. Problems of pad welding structural steels with martensitic filler material. *Adv. Mater. Sci.* **2019**, *19*, 5–14. [CrossRef]
52. Tomków, J.; Rogalski, G.; Fydrych, D.; Łabanowski, J. Improvement of S355G10+N steel weldability in water environment by temper bead welding. *J. Mater. Process. Technol.* **2018**, *262*, 372–381. [CrossRef]
53. Sun, S.D.; Fabijanic, D.; Barr, C.; Liu, Q.; Walker, K.; Matthews, N.; Orchowski, N.; Easton, M.; Brandt, M. In-situ quench and tempering for microstructure control and enhanced mechanical properties of laser cladded AISI 420 stainless steel powder on 300M steel substrates. *Surf. Coat. Technol.* **2018**, *333*, 210–219. [CrossRef]
54. Jorge, J.C.F.; Monteiro, J.L.D.; de Carvalho Gomes, A.J.; de Souza Bott, I.; de Souza, L.F.G.; Mendes, M.C.; Araújo, L.S. Influence of welding procedure and PWHT on HSLA steel weld metals. *J. Mater. Res. Technol.* **2018**, *8*, 561–571. [CrossRef]
55. Rahman Rashid, R.A.; Abaspour, S.; Palanisamy, S.; Matthews, N.; Dargusch, M.S. Metallurgical and geometrical characterisation of the 316L stainless steel clad deposited on a mild steel substrate. *Surf. Coat. Technol.* **2017**, *327*, 174–184. [CrossRef]
56. Rahman Rashid, R.A.; Nazari, K.A.; Barr, C.; Palanisamy, S.; Orchowski, N.; Matthews, N.; Dargusch, M.S. Effect of laser reheat post-treatment on the microstructural characteristics of laser-cladded ultra-high strength steel. *Surf. Coat. Technol.* **2019**, *372*, 93–102. [CrossRef]
57. Lisiecki, A.; Ślizak, D. Hybrid laser deposition of Fe-based metallic powder under cryogenic conditions. *Metals* **2020**, *10*, 190. [CrossRef]
58. Alipooramirabad, H.; Paradowska, A.; Ghomashchi, R.; Reid, M. Investigating the effects of welding process on residual stresses, microstructure and mechanical properties in HSLA steel welds. *J. Manuf. Process.* **2017**, *28*, 70–81. [CrossRef]